Bright Green Upconversion Fluorescence of Yb^{3+}, Er^{3+}-codoped Fluoride Colloidal Nanocrystal and Submicrocrystal Solutions

Yan Wang,[2] Weiping Qin,*[1,2] Jisen Zhang,[2] Chunyan Cao,[2] Jishuang Zhang,[2] Ye Jin,[2] Peifen Zhu,[1] Guodong Wei,[1] Guofeng Wang,[1] and Lili Wang[1]

[1]*State Key Laboratory of Integrated Optoelectronics, College of Electronic Science & Engineering, Jilin University, Changchun 130012, P. R. China*

[2]*Key Laboratory of Excited State Processes, Changchun Institute of Optics, Fine Mechanics and Physics, Chinese Academy of Sciences, Changchun 130033, P. R. China*

(Received March 22, 2007; CL-070308; E-mail: wpqin@jlu.edu.cn)

Hexagonal-phase LaF_3: Yb^{3+}, Er^{3+}, hexagonal-phase $NaGdF_4$: Yb^{3+}, Er^{3+}, cubic-phase $NaYF_4$: Yb^{3+}, Er^{3+} nanocrystals (NCs), and hexagonal-phase $NaYF_4$: Yb^{3+}, Er^{3+} submicrorods (MRs) were prepared with oleic acid as capping ligand. The NCs and MRs can be redispersed in nonpolar organic solvents, thus forming transparent and stable solutions. Under a 980-nm excitation from a diode laser, the Yb^{3+}, Er^{3+}-codoped NC and MR colloidal solutions present bright green upconversion fluorescence.

In recent years, with rapidly shrinking in size, lanthanide-doped upconversion nanocrystalline and submicrocrystalline materials have attracted considerable attentions owing to their potential applications in optics,[1] communication,[2] catalysis fields,[3] and biological labeling.[4] It is well known that the luminescence of lanthanide-doped upconversion phosphors is very easily quenched by high energy vibrations originated from host materials and water molecules and that fluorides materials with low phonon energy[4–6] are usually used as the host matrices to increase the efficiency of upconversion luminescence. Although much work has been done on lanthanide-doped fluoride upconversion nanocrystalline and submicrocrystalline materials, most of them focused on solid-state materials. In order to realize the biological imaging or display applications based on the upconversion principle in a fluid, it is crucial to investigate lanthanide-doped upconversion nanocrystalline and submicrocrystalline colloidal solutions. To date, however, the successful preparation of transparent colloidal solutions has only been demonstrated in a limited number of $NaYF_4$ samples.[4,7–12] Others, such as LaF_3 and $NaGdF_4$ have not been reported, to our knowledge. Herein, we report a study on four transparent Yb^{3+}, Er^{3+}-codoped fluoride nanocrystalline and submicrocrystalline colloidal solutions. Under a 980-nm excitation from a laser diode, the transparent solutions present bright green upconversion fluorescence.

In a typical preparation, 2.4 g of NaOH was dissolved in a solution containing oleic acid, ethanol, and deionized water (10/5/1, v/v). Then, 4 mL of 1.5 or 3 M KF and 4 mL of deionized water containing 1.56 mmol $Ln(NO_3)_3 \cdot 6H_2O$ (Ln = La, Gd, or Y), 0.40 mmol $Yb(NO_3)_3 \cdot 6H_2O$ and 0.04 mmol $Er(NO_3)_3 \cdot 6H_2O$ were added into above solution under vigorous stirring. The mixture was agitated for 30 min and then transferred into four 50-mL autoclaves which are sealed and treated at 160–180 °C for 8–16 h. Subsequently, the mixture was allowed to cool to room temperature, and the powder were obtained by centrifuge, rinse and drying.

The size and morphology of NCs and MRs were characterized by TEM (JEM, 2000EX 200 kV). Phase identification was performed via X-ray diffractometry (model Rigaku RU-200b), using nickel-filtered Cu Kα radiation ($\lambda = 1.5406$ Å). FT-IR spectra within the range of 4000–400 cm^{-1} were recorded by a Bio-Rad Fourier transform infrared spectrometer with the KBr pellet technique. The upconversion emission spectra were taken with a Hitachi F-4500 fluorescence spectrometer. A 980-nm laser diode (2 W) was used as the excitation source. The upconversion luminescence of colloidal solution was acquired with a digital camera. The time exposure was 6 s.

Figure 1 shows the XRD patterns of powder. The position and intensity of the diffraction peaks of four samples are in good agreement with the standard value for bulk hexagonal-phase LaF_3 (JCPDS No. 84-0942), hexagonal-phase $NaGdF_4$ (No. 27-0699), cubic-phase $NaYF_4$ (No. 77-2024), and hexagonal-phase $NaYF_4$ (No. 16-0334), respectively. The broadening of the diffraction peaks is attributed to the small particle size and the overlapping of the diffraction peaks. The XRD also demonstrates that under the similar experimental conditions, the Na ions can be incorporated into the framework of LnF_n (Ln = Gd and Y), forming $NaGdF_4$ and $NaYF_4$.

Figure 2 displays transmission electron microscopy (TEM) images of samples. For the LaF_3 NCs (Figure 2a), we can see that their diameters vary from 10 to 20 nm and that most particles present hexagonal profiles or show apparent crystal facets. TEM image of $NaGdF_4$ NCs also presents hexagonal profiles, and the particle size is about 20 nm (Figure 2b). Figure 2c shows the TEM image of cubic-phase $NaYF_4$ NCs, the particle size vary from 20 to 40 nm, and the particles are not ideally spherical. With increase of F^- ion concentration, temperature and reactive

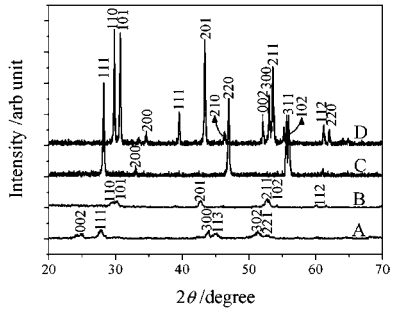

Figure 1. Powder XRD patterns of (A) hexagonal-phase LaF_3: Yb^{3+}, Er^{3+}, (B) hexagonal-phase $NaGdF_4$: Yb^{3+}, Er^{3+}, (C) cubic-phase $NaYF_4$: Yb^{3+}, Er^{3+}, and (D) hexagonal-phase $NaYF_4$: Yb^{3+}, Er^{3+}.

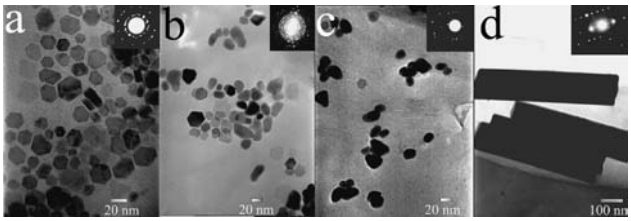

Figure 2. TEM images of (a) hexagonal-phase LaF_3: Yb^{3+}, Er^{3+}, (b) hexagonal-phase $NaGdF_4$: Yb^{3+}, Er^{3+}, (c) cubic-phase $NaYF_4$: Yb^{3+}, Er^{3+}, and (d) hexagonal-phase $NaYF_4$: Yb^{3+}, Er^{3+}. Insert: The corresponding electronic diffraction patterns of samples.

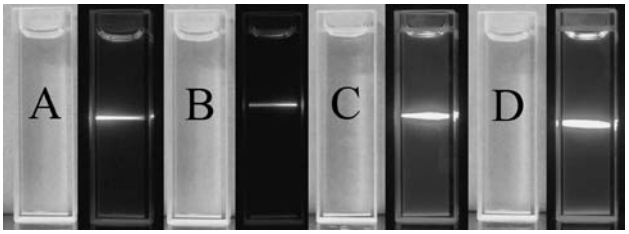

Figure 3. Photographs of (A) hexagonal-phase LaF_3: Yb^{3+}, Er^{3+}, (B) hexagonal-phase $NaGdF_4$: Yb^{3+}, Er^{3+}, (C) cubic-phase $NaYF_4$: Yb^{3+}, Er^{3+}, and (D) hexagonal-phase $NaYF_4$: Yb^{3+}, Er^{3+} dispersed in cyclohexane show eye-visible upconversion luminescence, under 980-nm excitation with the concentration of 2 mg/mL. Labeled cells demonstrate that the colloidal solutions are fully transparent (See the table of contents for color illustration).

time, the hexagonal-phase $NaYF_4$ MRs are formed (Figure 2d). The diameter of MRs is about 100–120 nm and the length is about 700 nm. The electronic diffraction (inset in Figures 2a–2d, respectively) further indicates that the samples are well crystallized.

Figure 3 shows photographs of hexagonal-phase LaF_3: Yb^{3+}, Er^{3+}, hexagonal-phase $NaGdF_4$: Yb^{3+}, Er^{3+}, cubic-phase $NaYF_4$: Yb^{3+}, Er^{3+} NCs, and hexagonal-phase $NaYF_4$: Yb^{3+}, Er^{3+} MRs in cyclohexane with the concentration of 2 mg/mL. These solutions are stable for months without any visible precipitate. The well dispersivity of the samples in cyclohexane is due to the oleic acid molecules coated onto the outer face of the nanocrystals. The surface modification of the nanocrystals with oleic acid was confirmed by FT-IR spectrum (Figure 4). The photographs show that the colloidal solutions are transparent, and under 980-nm excitation the solutions demonstrate eye-visible green upconversion luminescence with pump power density 125 W/cm^2.

The room temperature upconversion emission spectra of hexagonal-phase LaF_3: Yb^{3+}, Er^{3+}, hexagonal-phase $NaGdF_4$: Yb^{3+}, Er^{3+}, cubic-phase $NaYF_4$: Yb^{3+}, Er^{3+} NCs, and hexagonal-phase $NaYF_4$: Yb^{3+}, Er^{3+} MRs are presented in Figure 5. Under 980-nm excitation, four emission peaks in the visible range are assigned to $^2H_{9/2} \rightarrow {}^4I_{15/2}$ (407 nm), $^2H_{11/2} \rightarrow {}^4I_{15/2}$ (520 nm), $^4S_{3/2} \rightarrow {}^4I_{15/2}$ (538 nm), and $^4F_{9/2} \rightarrow {}^4I_{15/2}$ (651 nm) transitions of Er^{3+} ions, respectively. Except visible emissions, violet emission of Er^{3+} ions also presents in the emission spectra, corresponding to the transition of $^4G_{11/2} \rightarrow {}^4I_{15/2}$ (380 nm). The emission spectra also show that under exactly the same Yb^{3+} and Er^{3+} composition, solution concentration and pump power density, the emission light outputs of hexagonal-phase $NaYF_4$: Yb^{3+}, Er^{3+} MRs, cubic-phase $NaYF_4$: Yb^{3+}, Er^{3+} and

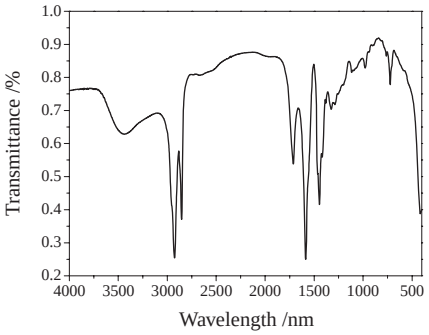

Figure 4. FT-IR spectrum of hexagonal-phase LaF_3: Yb^{3+}, Er^{3+}.

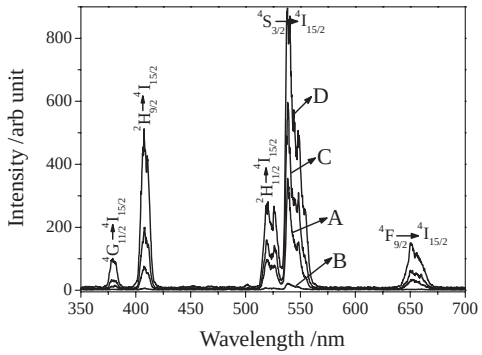

Figure 5. Upconversion emission spectra of colloidal solutions. (A) hexagonal-phase LaF_3: Yb^{3+}, Er^{3+}, (B) hexagonal-phase $NaGdF_4$: Yb^{3+}, Er^{3+}, (C) cubic-phase $NaYF_4$: Yb^{3+}, Er^{3+}, and (D) hexagonal-phase $NaYF_4$: Yb^{3+}, Er^{3+}.

hexagonal-phase LaF_3: Yb^{3+}, Er^{3+} NCs, estimated by fitting the area under the emission bands, were about 23.76, 11.85, 6.53 times higher than that of hexagonal-phase $NaGdF_4$: Yb^{3+}, Er^{3+} NCs, respectively. These shifts may be due to the difference in particle size, host geometry, phonon energy, and so on.

In conclusion, four Yb^{3+}, Er^{3+}-codoped fluoride nanocrystals and submicrocrystals were synthesized. These crystals demonstrate high crystal quality and excellent dispersivity and can be transparently dispersed in nonpolar solvents. At the same time, the transparent colloidal solutions show efficient infrared-to-violet and infrared-to-visible upconversion emissions. These crystals have potential applications in biosensors, display, and short-wavelength lasers based on the upconversion principle.

This work is supported by National Science Foundation of China. (Grant Nos. 10474096 and 50672030).

References

1 K. Riwotzki, H. Meyssamy, H. Schnablegger, A. Kornowski, M. Haase, *Angew. Chem., Int. Ed.* **2001**, *40*, 573.
2 J. W. Stouwdam, F. C. J. M. van Veggel, *Nano Lett.* **2002**, *2*, 733.
3 K. Zhou, X. Wang, X. M. Sun, Q. Peng, Y. Li, *J. Catal.* **2005**, *229*, 206.
4 S. Heer, K. Kömpe, H. U. Güdel, M. Haase, *Adv. Mater.* **2004**, *16*, 2102.
5 G. J. H. De, W. Qin, J. Zhang, D. Zhao, J. Zhang, *Chem. Lett.* **2005**, *34*, 914.
6 R. Yan, Y. Li, *Adv. Funct. Mater.* **2005**, *15*, 763.
7 J. C. Boyer, F. Vetrone, L. A. Cuccia, J. A. Capobianco, *J. Am. Chem. Soc.* **2006**, *128*, 7444.
8 G. S. Yi, G. M. Chow, *Adv. Funct. Mater.* **2006**, *16*, 2324.
9 L. Y. Wang, Y. Li, *Nano Lett.* **2006**, *6*, 1645.
10 Z. Q. Li, Y. Zhang, *Angew. Chem., Int. Ed.* **2006**, *45*, 7732.
11 G. S. Yi, G. M. Chow, *Chem. Mater.* **2007**, *19*, 341.
12 L. Wang, Y. Li, *Chem. Mater.* **2007**, *19*, 727.

Published on the web (Advance View) June 16, 2007; doi:10.1246/cl.2007.912